ORIGINAL PAPER

Vitronectin is Involved in the Morphological Transition of Neurites in Retinoic Acid-Induced Neurogenesis of Neuroblastoma Cell Line Neuro2a

Miyaka Sugahara[1] · Yuri Nakaoki[1] · Ayano Yamaguchi[1] · Kei Hashimoto[2] · Yasunori Miyamoto[1,2]

Abstract

Vitronectin (Vtn), one of the extracellular matrix proteins, has been reported to result in cell cycle exit, neurite formation, and polarization of neural progenitor cells during neurogenesis. The underlying mechanism, however, has not been fully understood. In this study, we investigated the roles of Vtn and its integrin receptors, during the transition of neurites from multipolar to bipolar morphology, accompanying the cell cycle exit in neural progenitor cells. We used mouse neuroblastoma cell line Neuro2a as a model of neural progenitor cells which can induce cell cycle exit and the morphological transition of neurites by retinoic acid (RA)-stimulation. Treatment with an antibody for Vtn suppressed the RA-induced cell cycle exit and multipolar-to-bipolar transition. Furthermore, immunostaining results showed that in the cells displaying multipolar morphology Vtn was partially localized at the tips of neurites and in cells displaying bipolar morphology at both tips. This Vtn localization and multipolar-to-bipolar transition was perturbed by the transfection of a dominant negative mutant of cell polarity regulator Par6. In addition, a knockdown of β5 integrin, which is a receptor candidate for Vtn, affected the multipolar-to-bipolar transition. Taken together, these results suggest that Vtn regulates the multipolar-to-bipolar morphological transition via αvβ5 integrin.

Keywords Vitronectin · Integrin · Morphological transition · Cell cycle

Abbreviations

Vtn	Vitronectin
RA	Retinoic acid
CGCP	Cerebellar granule cell precursor
DAPI	4′,6-Diamidino-2-phenylindole, dihydrochloride
BrdU	5-Bromodeoxyuridine
siRNA	Short-interfering RNA

Introduction

The size and shape of the cerebellar and cerebral cortex are regulated by the organization and behavior of neural progenitor cells during development [1, 2]. The morphological transition, polarization, migration, and neurite formation of these neural progenitor cells proceed spatiotemporally, accompanied with cell cycle exit [3–5]. In the developing cerebellum, cerebellar granule cell precursors (CGCPs) proliferating in the outer external granular layer display multipolar morphology with several short protrusions [5]. After cell cycle exit, CGCPs migrate into the inner external granular layer and change the shape from multipolar to bipolar morphology [5]. The behavior of CGCPs is regulated by several external factors, including extracellular matrix proteins.

Vitronectin (Vtn), one of the extracellular matrix proteins, is transiently expressed in the developing brain and is known to have various functions in the developing nervous system [6, 7]. In the early stages of motor neuron differentiation of chick embryos, Vtn is expressed in the floor plate of neural tubes, and treatment with the Vtn antibody reduces the number of motor neurons [8, 9]. Vtn also plays a role in the survival and differentiation of retinal optic nerve cells of chick embryos [10]. Furthermore, Vtn promotes the nerve growth factor-dependent neurite elongation in PC12 cells [11].

✉ Yasunori Miyamoto
miyamoto.yasunori@ocha.ac.jp

1 Graduate School of Humanities and Sciences, Ochanomizu University, Otsuka 2-1-1, Bunkyo-ku, Tokyo, Japan

2 Institute for Human Life Innovation, Ochanomizu University, Otsuka 2-1-1, Bunkyo-ku, Tokyo, Japan

It has been reported that Vtn contributes to the regulation of proliferation, differentiation and neurite elongation in mouse CGCPs. In the primary culture of mouse CGCPs, Vtn suppresses proliferation and promotes differentiation [12]. The antibody for αvβ5 integrin, one of the Vtn receptors, suppresses the neurite elongation of CGCPs [13]. In addition, it has been reported that Vtn regulates the position of centrosomes in cultured CGCPs, indicating that Vtn may be involved in cell polarity [14]. We previously found that Vtn promotes the progress of the initial differentiation stage in mouse CGCPs through αvβ5 integrin [15]. In addition, we observed that the addition of Vtn promotes the cell cycle exit of cultured CGCPs [16]. During the development of the cerebellum, the transition from multipolar to bipolar morphology is accompanied with cell cycle exit in CGCPs [5]. However, it is unknown whether Vtn is involved in the transition of neurites from multipolar to bipolar morphology in neural progenitor cells.

One of mouse neuroblastoma cell lines, Neuro2a, is known as a retinoic acid (RA)-induced neurogenesis model. Some studies show that RA induces morphological transitions of neurites and cell cycle exit [17, 18]. We previously reported that the expression of Vtn protein transiently increases during RA-induced neural differentiation of Neuro2a cells [19].

In this study, we analyzed the effect of Vtn on the morphological transition of neurites in RA-stimulated Neuro2a cells. Our analysis revealed that Vtn promotes the RA-induced transition from multipolar to bipolar morphology, accompanied by cell cycle exit in Neuro2a cells. Furthermore, cell polarity regulator Par6 and Vtn receptor αvβ5 integrin contribute to the regulation of the RA-stimulated multipolar-to-bipolar morphological transition by Vtn.

Materials and Methods

Cell Culture and RA Stimulation

Mouse neuroblastoma Neuro2a cells were obtained from Riken Cell Bank (Tsukuba, Japan). Neuro2a cells were grown in Minimum Essential Medium Eagle (MEM, Sigma-Aldrich, St. Louis, MO) supplemented with 10% fetal bovine serum, 1% non-essential amino acids (NEAA) (Thermo Fisher Scientific, Waltham, MA) and 1% Penicillin–Streptomycin (PS) (Thermo Fisher Scientific). Cells were cultured in poly-L-Lysine-coated (Sigma-Aldrich) 24-well plates (1.5×10^4 or 3.0×10^4 cells/well) in 5% CO_2 at 37 °C overnight. Next, the medium was replaced with serum-free medium (MEM, 1% insulin-transferrin-selenium solution (Thermo Fisher Scientific), 1% NEAA and 1% PS) supplemented with RA (10-15 µM) and cultured for 2 days more.

Quantitative Real-Time Reverse Transcription (RT)-PCR

Total RNA was isolated from Neuro2a cells using TRIzol (Thermo Fisher Scientific) and then reverse-transcribed using a ReverTra Ace qPCR RT Kit (TOYOBO, Osaka, Japan) as described by the manufacturer. The cDNAs for Vtn, β5 integrin, and internal control GAPDH were amplified using the following specific primers: Vtn forward, 5′-TTCTCTGGCTGACCAAGAGTCA-3′, Vtn reverse, 5′-AAGTACCGGTCGTTCTTCAC-3′, β5 integrin forward, 5′-GCCTGTTGATCCACCCAAAAT-3′, β5 integrin reverse, 5′-CGTTGAGTGCCAGGTAGTG-3′, GAPDH forward, 5′-CGTGTTCCTACCCCCAATGT-3′, and GAPDH reverse, 5′-TCTTTGGCAGGTTCATACTACTGT-3′. PCR was performed using KOD SYBR qPCR Mix (TOYOBO) as described by the manufacturer. Real-time PCR was performed on an ABI 7300 real-time PCR machine (Thermo Fisher Scientific): after denaturation for 2 min at 98 °C, amplification was performed with 40 cycles of 10 s at 98 °C, 10 s at 60 °C, and 30 s at 68 °C. The data were analyzed using the delta Ct method. The expression level was normalized to GAPDH expression.

Western Blotting

Neuro2a cells were lysed in RIPA buffer (BioDynamics Laboratory, Inc., Tokyo, Japan). Cell lysates were subjected to 10% SDS-PAGE and transferred onto polyvinylidene difluoride membranes (ATTO, Tokyo, Japan) for 1 h at 80 mA. The membranes were blocked with TBS-T (25 mM Tris–HCl (pH 7.5), 150 mM NaCl, 0.1% Tween-20) containing 0.35% skim milk overnight. The membranes were incubated with primary antibodies against vitronectin (1:2500, gift from Dr. Masao Hayashi) or β-actin (1:5000, G043, Applied Biological Materials, Inc., BC, Canada) for 1 h each. After washing in TBS-T, the membranes were incubated with horseradish peroxidase-conjugated anti-rabbit or anti-mouse IgG antibodies (1:5000, Cell Signaling Technology, Inc., Danvers, MA) for 1 h and washed again. To detect immunoreactivity, the blots were incubated with enhanced chemiluminescent reagent (EzWestLumiOne, ATTO), and images were captured with an ImageQuant LAS 4000 (GE Healthcare, Little Chalfont, UK). The protein size was determined using pre-stained Protein Markers (Nakarai Tesque, Kyoto, Japan).

Vtn-Inhibition and Vtn-Addition Experiments

Vtn antibody and rabbit immunoglobulin G (IgG), generated by Dr. Hayashi [20], were added to an overnight culture of Neuro2a cells to each well (10 µg/ml) for the Vtn-inhibition

experiments. It has been reported that the Vtn antibody used in this study specifically binds to mouse Vtn [20]. Recombinant human Vtn protein (final concentration of 5 µg/ml, hRP-0299, LD BioPharma, Inc., San Diego, CA) or 0.2 µM Tris–HCl solution as a vehicle was added to the culture media for Vtn-addition experiments. In order to investigate the efficiency of cell cycle exit, cells were treated with 5-bromodeoxyuridine (BrdU) 24 h after RA addition. BrdU can trace the fraction of cells passing through the S-phase. The cells were fixed 24 h after BrdU-introduction.

Knockdown Experiments Using Short-Interfering RNA

For knocking down mouse Vtn, β3 and β5 integrins, short-interfering RNAs (siRNA) for Vtn, β3, and β5 integrins (Stealth RNAi™ siRNA, Thermo Fisher Scientific) and control siRNAs (negative control Hi GC, Med GC or Lo GC, Thermo Fisher Scientific) were introduced into Neuro2a cells. For the introduction of the siRNAs, a mixture of 0.5 µl Lipofectamine 2000 Transfection Reagent (Thermo Fisher Scientific) and 1.5 µl of each siRNA (30 pmol) in 100 µl of Opti-MEM Reduced Serum Medium (Thermo Fisher Scientific) was added to each well of a 24-well plate and incubated for 5 h.

Transfection of Vectors

Integrin expression plasmid vectors (pCMV6-XL-β3 integrin, pCMV6-XL-β5 integrin, or pCMV6-XL plasmid vector) were obtained from OriGene (Rockville, MD). A dominant negative Par6 (pCMV5 Flag-Par6 delta 250-295 Flag tagged vector) and wild-type Par6 (pCMV5B-Flag-Par6 wt vector) expression plasmid vector were obtained from Addgene (Watertown, MA). To generate an empty vector for dominant negative and wild-type Par6 expression vectors, the pCMV5B-Flag-Par6 wt vector was digested with ClaI and XbaI, and the vector fragment was isolated. Next, the vector fragment was ligated with the fragment containing the sequence of FLAG (forward: 5′-cgataccatggactacaa ggacgacgatgacaagggttaat-3′ and reverse: 5′-ctagattaacccttg tcatcgtcgtccttgtagtccatggtat-3′). To transfect the vectors, a mixture of 0.5 µl Lipofectamine 2000 Transfection Reagent and 0.5 µg of each vector in 100 µl of Opti-MEM Reduced Serum Medium was added to each well of a 24-well plate and incubated for 5 h.

Immunofluorescence Staining

Immunostaining of Neuro2a cells was performed as follows. The fixed cells were washed with phosphate buffered saline and then blocked with a blocking buffer (10% calf serum, 3% bovine serum albumin, 130 nM glycine, 0.4% Triton-X100

in Tris-buffered saline). The cells were incubated with the primary antibody overnight, and then with the secondary antibody for 1 h in the dark. The primary antibodies in this study included: anti-BrdU (1:500; MAB3222; Merck Millipore, Darmstadt, Germany), anti-Ki67 (1:200; RM9106-S0; Thermo Fisher Scientific), anti-vitronectin (1:500; LSL-LB-2096; Cosmo Bio, CA), anti-β3 integrin (1:200; sc-14009; Santa Cruz Biotechnology, Dallas, TX), anti-β5 integrin (1:250; sc-398214; Santa Cruz Biotechnology), anti-Par3 (1:50; sc-53819; Santa Cruz Biotechnology), anti-Par6 (1:50; sc-365323; Santa Cruz Biotechnology) and anti-Flag (1:1000; F1804; Sigma-Aldrich). The secondary antibodies in this study included: Alexa Fluor 488 goat anti-mouse IgG (1:200), Alexa Fluor 488 goat anti-rabbit IgG (1:200), Alexa Fluor 568 goat anti-mouse IgG (1:200), Alexa Fluor 568 goat anti-rabbit IgG (1:200) and Alexa Fluor 568 Phalloidin (1:40) (Thermo Fisher Scientific). For staining with anti-BrdU and anti-Ki67 antibodies, the cells were boiled in 10 mM citrate buffer (pH 6.0) prior to blocking. Following antibody staining, the cells were stained with 0.5 µg/ml 4′,6-diamidino-2-phenylindole dihydrochloride (DAPI) (Roche Diagnostics, Basel, Switzerland) in Tris-buffered saline. Images were captured using a microscope (FSX100, Olympus, Tokyo, Japan) or confocal laser scanning microscope (LSM700, Carl Zeiss, Oberkochen, Germany).

RT-PCR

Total RNA was isolated from Neuro2a cells at 48 h after stimulation with 10 µM RA and then reverse-transcribed as described above. cDNA was amplified by PCR using GoTaq Green Master Mix (Promega, Madison, WI) and specific primers for each integrins: β1 integrin forward, 5′-AACTGCACCAGCCCATTTAG-3′, β1 integrin reverse, 5′-AACCTAAGAGGTCTTCCACC-3′, β3 integrin forward, 5′-CATCCAGACCCTGGGTACCA-3′, β3 integrin reverse, 5′-TGATCGTTGGAAGCCTAACCG-3′, β5 integrin forward, 5′-GCCTGTTGATCCACCCAAAAT-3′, β5 integrin reverse, 5′-CGTTGAGTGCCAGGTAGTG-3′, GAPDH forward, 5′-CGTGTTCCTACCCCCAATGT-3′ and GAPDH reverse, 5′-TCTTTGGCAGGTTCATACTACTGT-3′. The amplification program comprised one cycle at 92 °C for 5 min, followed by 40 cycles at 92 °C for 1 min, 60 °C for 1 min, 72 °C for 1 min, with a final extension at 72 °C for 7 min. The PCR products were separated by electrophoresis on 1.8% TAE agarose gels and visualized by ethidium bromide staining.

Analysis of Neurite Morphology

To analyze the morphological transition, Neuro2a cells were fixed with 4% paraformaldehyde in 0.2 M phosphate buffered saline. Images were obtained using a phase-contrast

microscope (FSX100, Olympus). Depending on the number of neurites, we classified neurite morphology into four groups. Groups containing cells without neurites, with one, two, and three or more neurites were classified as nonpolar, monopolar, bipolar, and multipolar morphologies, respectively. The number of neurites was determined using Adobe Photoshop software (Adobe Inc., San Jose, CA) as previously reported [18]. Time-lapse imaging was used to investigate the influence of knockdown of β5 integrin on morphological changes in neurites. Images were obtained at 15-min intervals for 48 h from the medium exchange after transfection of siRNA and RA treatment by using an IncuCyte S3 Live-Cell Analysis System (Essen BioScience, Ann Arbor, MI).

Co-localization Analysis

To analyze the co-localization of Vtn and Par3/Par6, Neuro2a cells were stained with anti-Vtn and anti-Par3 or anti-Par6 antibodies. The images were captured using a confocal laser scanning microscope (LSM700, Carl Zeiss). From the obtained fluorescence images, scatterplots with the intensity of Par3 or Par6 on the Y-axis and Vtn on the X-axis were created using ZEN imaging software. After setting the threshold of fluorescence intensity of each channel, pixels with fluorescence intensity in excess of the threshold value were regarded as co-localized regions. The co-localized regions including the intensity information of both Vtn and Par3/Par6 were displayed with white pixels in the fluorescence images.

Hoechst Staining

To analyze the influence of β5 integrin knockdown on cell viability from the perspective of nuclear morphology, Neuro2a cells were transfected with control siRNA or β5 integrin siRNA, and stained at 12 h intervals for 48 h from the medium exchange after transfection of siRNA and RA treatment. Hoechst staining was performed as follows: after removing the culture medium, the cells were incubated with Hoechst 33342 solution (diluted to 1 µg/ml with phosphate buffered saline) (Dojindo Laboratories, Kumamoto, Japan) for 15 min at 37 °C. Fluorescence and phase contrast images were captured by using a microscope (FSX100). The nuclear morphology was observed to determine whether apoptosis was induced. Cell viability was calculated by counting the number of cells with normal nuclear morphology.

Statistical Analysis

At least three independent experiments were performed, and the data were analyzed using unpaired t test and ANOVA.

The results are expressed as the mean $\pm$ standard error of the mean and p values < 0.05 were considered significant.

Results

Expression Levels of Vtn are Up-Regulated by RA Treatment

First, we examined the effect of RA treatment on the Vtn protein expression level. Western blot analysis showed that the expression level of Vtn protein was increased in the cell lysate of Neuro2a cells at 12 h after RA treatment (Fig. 1a, b). Next, we examined the expression levels of *Vtn* mRNA in Neuro2a cells. Real-time RT-PCR revealed that the expression levels of *Vtn* mRNA transiently increased at 5 h after RA treatment and returned to the RA-nontreated level at 24 h after RA treatment (Fig. 1c).

Inhibition of Vtn Suppresses RA-Induced Cell Cycle Exit in Neuro2a Cells

RA is known to promote the cell cycle exit and elongate neurites of Neuro2a cells. To examine the effect of Vtn on the RA-induced cell cycle exit of Neuro2a cells, we carried out Vtn inhibition experiments using an antibody against Vtn. To trace the cells passing from the S-phase to cell cycle exit, BrdU was incorporated into Neuro2a cells in S-phase at 24 h before fixation. Using a cell cycling marker, Ki67, the efficiency of cell cycle exit was determined as the ratio of BrdU-positive and Ki67-negative (BrdU+;Ki67−) cells to BrdU-positive cells within 24 h before fixation. BrdU and Ki67 double-negative cells shown in Fig. 1d with bipolar morphology passed S-phase before BrdU incorporation and exited the cell cycle before fixation. The Vtn antibody significantly reduced the efficiency of the cell cycle exit compared to rabbit IgG (Fig. 1e). In contrast, addition of exogenous Vtn to the medium significantly increased the efficiency of cell cycle exit (Fig. 1f, g). To examine whether the morphology of neurites was correlated with the BrdU/Ki67 expression level, phase contrast images corresponding to the same field of fluorescence images were obtained (Fig. 1d, f). The images showed that many BrdU+; Ki67+ and BrdU+; Ki67- cells had multipolar and bipolar morphologies, respectively.

RA-Induced Neurite Morphological Transition is Linked to Cell Cycle Exit in Neuro2a Cells

Next, the relationship between RA-induced cell cycle exit and neurite morphology in Neuro2a cells was examined. The cell proliferation and morphology were examined at 0, 3, 7, 24 and 48 h after RA stimulation (RA+) and no stimulation (RA−). In the absence of RA, most Neuro2a
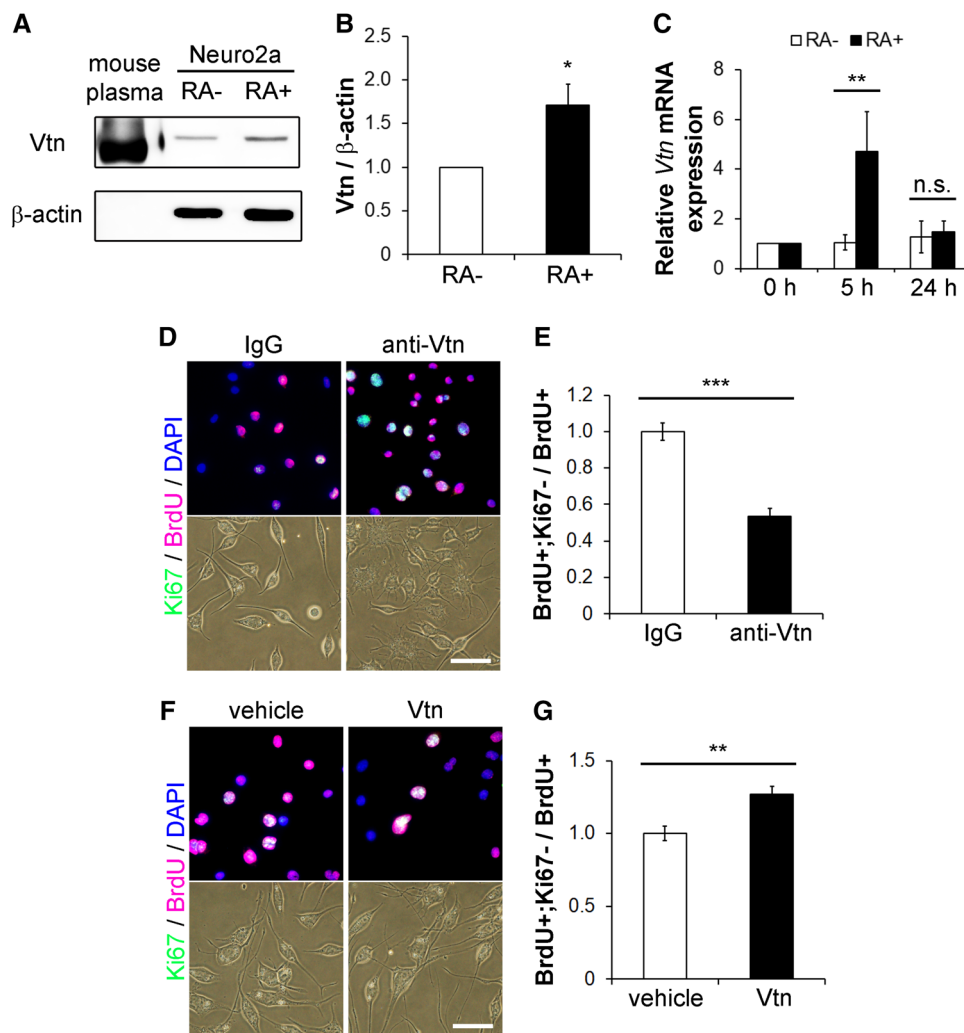
Fig. 1 Up-regulated Vtn expression by RA promotes cell cycle exit in Neuro2a cells. **a**, **b** Expression levels of Vtn protein with or without RA. Cell lysates were prepared from cells treated with 15 µM RA for 12 h and examined by western blotting using anti-Vtn antibody. β-actin was used as a loading control. Mouse plasma was used as a positive control for Vtn. Significance was calculated with unpaired t test. **c** Expression levels of *Vtn* mRNA with or without RA. Total RNA was isolated from cells after stimulation with 18 µM RA for 0, 5, and 24 h. Each mRNA level was quantified by real-time RT-PCR. Data were normalized to cells at 0 h after stimulation. Significance was calculated by ANOVA. Data were normalized to cells without RA. **d–g** Cells (3.0×10^4 cells/well) were treated with the antibody against Vtn and normal rabbit IgG (10 µg/ml) (**d**, **e**), or recombinant human Vtn protein (5 µg/ml) and 0.2 µM Tris–HCl solution as a vehicle (**f**, **g**) synchronized with RA stimulation (15 µM). **d**, **f** Representative images of phase-contrast and cells after immunofluorescence staining for BrdU (red), Ki67 (green), and DAPI (blue). The cells were labeled with BrdU for 24 h. **e**, **g** The effect of the Vtn-antibody or recombinant Vtn protein on cell cycle exit. The efficiency of the cell cycle exit is calculated as the percentage of cells that exited the cell cycle (BrdU+; Ki67−) divided by total BrdU-positive cells (BrdU+). Data were normalized to cells treated with rabbit IgG or Tris–HCl solution, respectively. Significance was calculated with unpaired t test; *$p < 0.05$, **$p < 0.01$, ***$p < 0.001$. Data are mean ± SEM of three independent experiments. Scale bar = 50 µm (Color figure online)

cells displayed multipolar morphology and continued to proliferate (Fig. 2a). Neurite elongation and the transition from multipolar to bipolar morphology were both observed to be time-dependent in RA+ cells. Cells treated with RA for 24 h mainly displayed multipolar morphology (approximately 70% of the total cell number), while those after 48 h of treatment mainly displayed bipolar morphology (approximately 70% of the total cell number) (Fig. 2b). In cells treated with RA for 48 h, approximately 70% of Ki67-positive (Ki67 +) cells showed multipolar morphology, while approximately 70% of Ki67-negative (Ki67−) cells showed bipolar morphology (Fig. 2c). This demonstrates the relevance to cell cycle exit and neurite morphology in Neuro2a cells. These results suggest that RA stimulation induces the transition of the neurites from multipolar to bipolar morphology to be associated with cell cycle exit in Neuro2a cells.

Fig. 2 RA induces the morphological transition of neurites associated with cell cycle exit in Neuro2a cells. **a** Representative images of the cells stimulated with 10 μM RA (RA+; 3.0×10^4 cells/well) or ethanol (RA−; 1.5×10^4 cells/well) at five time points (0, 3, 7, 24 and 48 h). **b** Temporal change in the proportion of cells displaying each neurite morphology. Cells were stimulated with 10 μM RA for 24 or 48 h. **c** Proportion of Ki67-positive (Ki67+) or Ki67-negative (Ki67−) cells displaying each neurite morphology. Cells stimulated with 10 μM RA for 48 h were stained with Ki67 and DAPI and counted by overlaying fluorescence images and phase-contrast images. Significance was calculated with ANOVA; **$p < 0.01$, ***$p < 0.001$. Data are mean ± SEM of three independent experiments. Scale bar = 50 μm
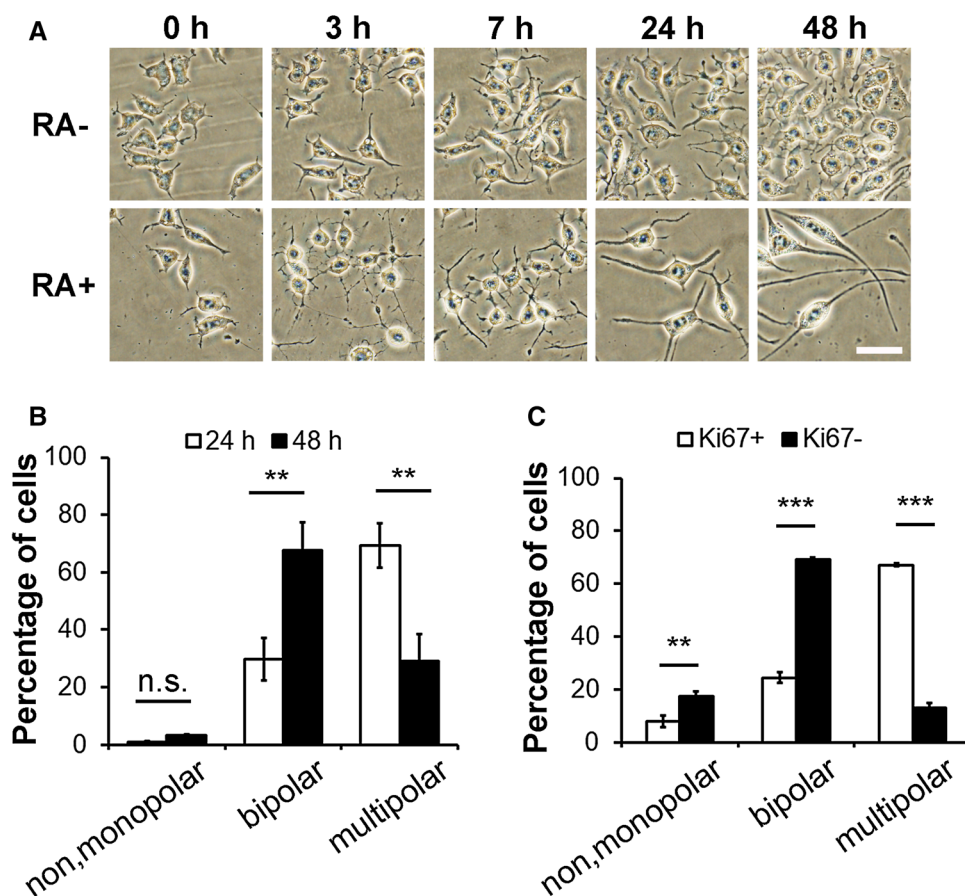
Localization of Vtn at Neurite Tips of Neuro2a Cells is Involved in the RA-Induced Morphological Transition of Neurites

To investigate the localization of Vtn during the morphological transition of neurites in Neuro2a cells, we performed an immunofluorescence staining of Vtn. In cells displaying multipolar morphology after RA treatment, Vtn was localized at the tips of some neurites. However, they did not always co-localize with Vtn and some neurite tips were Vtn-negative (Fig. 3a, c). On the other hand, Vtn was localized at both neurite tips in most cells displaying bipolar morphology (Fig. 3b, c). Further quantitative analysis of cells displaying multipolar morphology at 24 h after RA treatment showed two findings: (i) 23.6% and 36.1% of the cells had two and more than three Vtn-positive (Vtn+) neurites, respectively, (ii) 16.7% and 38.1% of the cells had two and more than three Vtn-negative (Vtn−) neurites, respectively (Fig. 3c–e).

To examine the effect of Vtn on the morphological transition of neurites, we carried out Vtn inhibition experiments, using an antibody against Vtn (Fig. 3f). Figure 3g shows that treatment with the Vtn antibody remarkably reduced the ratio of bipolar morphology and increased the ratio of

multipolar morphology. These data suggest that Vtn contributes to the RA-induced morphological transition of neurites in Neuro2a cells.

The Cell Polarity Regulator Par6 Contributes to Regulation of the Morphological Transition of Neurites by Vtn in Neuro2a Cells

It has been reported that the multipolar-to-bipolar morphological transition is mediated by a cell polarity regulator [21–23]. In addition, Par6/Par3/aPKC (Par complex) is known to serve as one of the cell polarity regulators [24, 25]. To examine the relationship between the Par complex and the regulation of the Vtn induced multipolar-to-bipolar morphological transition, we examined the localization of Par3 and Par6 using immunofluorescence staining and found that Par3 and Par6 were co-localized with Vtn at the tip of neurites (Fig. 4a, c). To confirm the co-localization between Vtn and Par3/Par6, we performed co-localization analysis. The fluorescence intensities of Vtn and Par3/Par6 in each pixel were plotted using scattergrams (the left panels of Fig. 4b, d). The pixels with both fluorescence intensities in the X-(Vtn) and Y-axes (Par3 or Par6) greater than the threshold value indicated the region that was co-localized
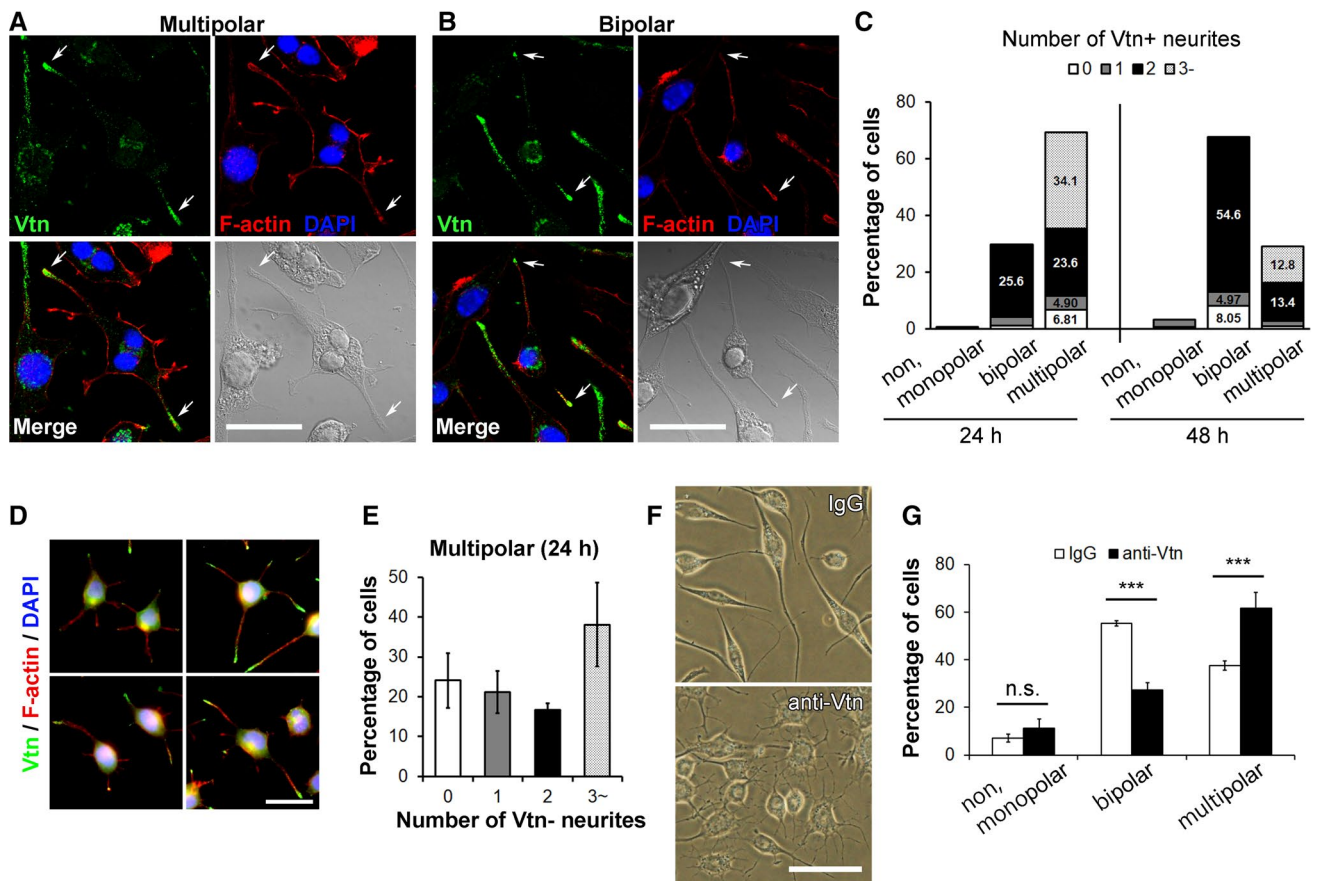
Fig. 3 Vtn localization at the tip of neurites is involved in the morphological transition of neurites in Neuro2a cells. Cells (3.0×10^4 cells/well) were stimulated with 10 μM RA for 48 h. Representative images of cells displaying multipolar (**a**) and bipolar (**b**) morphology after immunofluorescence staining for Vtn (green), F-actin (red) and DAPI (blue). Arrows indicate the localization of Vtn at the tip of neurites. Scale bar = 30 μm. **c** Number of Vtn-positive neurites in the cells displaying each neurite morphology. Cells were stimulated with RA for 24 or 48 h. **d** Fluorescence images of cells stimulated with 10 μM RA for 24 h. Scale bar = 30 μm. **e** Number of Vtn-negative (Vtn−) neurites in cells displaying multipolar morphology stimulated with 10 μM RA for 24 h. Scale bar = 30 μm. **f** Representative images of the cells treated with the Vtn antibody or normal rabbit IgG. Scale bar = 50 μml. **g** The proportion of cells displaying each neurite morphology. Significance was calculated with ANOVA; *$p < 0.05$, **$p < 0.01$, ***$p < 0.001$. Data are mean ± SEM of three independent experiments (Color figure online)

with Vtn and Par3/Par6. The pixels of the co-localization (white pixels) were localized at the tip of the neurites (the right panels in Fig. 4b, d). This result suggests that Par6 may be involved in the regulation of multipolar-to-bipolar transition by Vtn. To verify this hypothesis, we transfected Neuro2a cells with a dominant negative mutant of Par6. As a result, the transfection of the Par6 mutant (dnPar6) significantly decreased the fraction of bipolar morphology compared to the cells that were transfected with wild-type (WT) Par6 expression plasmid or empty vector plasmid as a mock control (mock: 72.8%, WT: 73.3%, dnPar6: 52.4%) (Fig. 4e). Furthermore, the transfection with dnPar6 perturbed the localization of Vtn at the neurite tips and eliminated the difference of the Vtn+ to Vtn− ratio in neurites (Fig. 4f). These results indicate that Par6 is involved in the regulation

of the transition from multipolar to bipolar morphology in RA-stimulated Neuro2a cells.

Contribution of αvβ5 Integrin to the Morphological Transition of Neurites, Accompanying the Cell Cycle Exit in Neuro2a Cells

To examine which integrin mediates the effect of Vtn on RA-induced cell cycle exit and morphological transition of neurites in Neuro2a cells, we investigated the mRNA expression level of αv, β1, β3, and β5 integrin using RT-PCR. This resulted in the amplification and the detection of PCR bands for these integrins (Fig. 5a). The localization of β3 and β5 integrins was confirmed with immunofluorescence staining (Fig. 5b, c). β3 integrin was localized in the cell body and
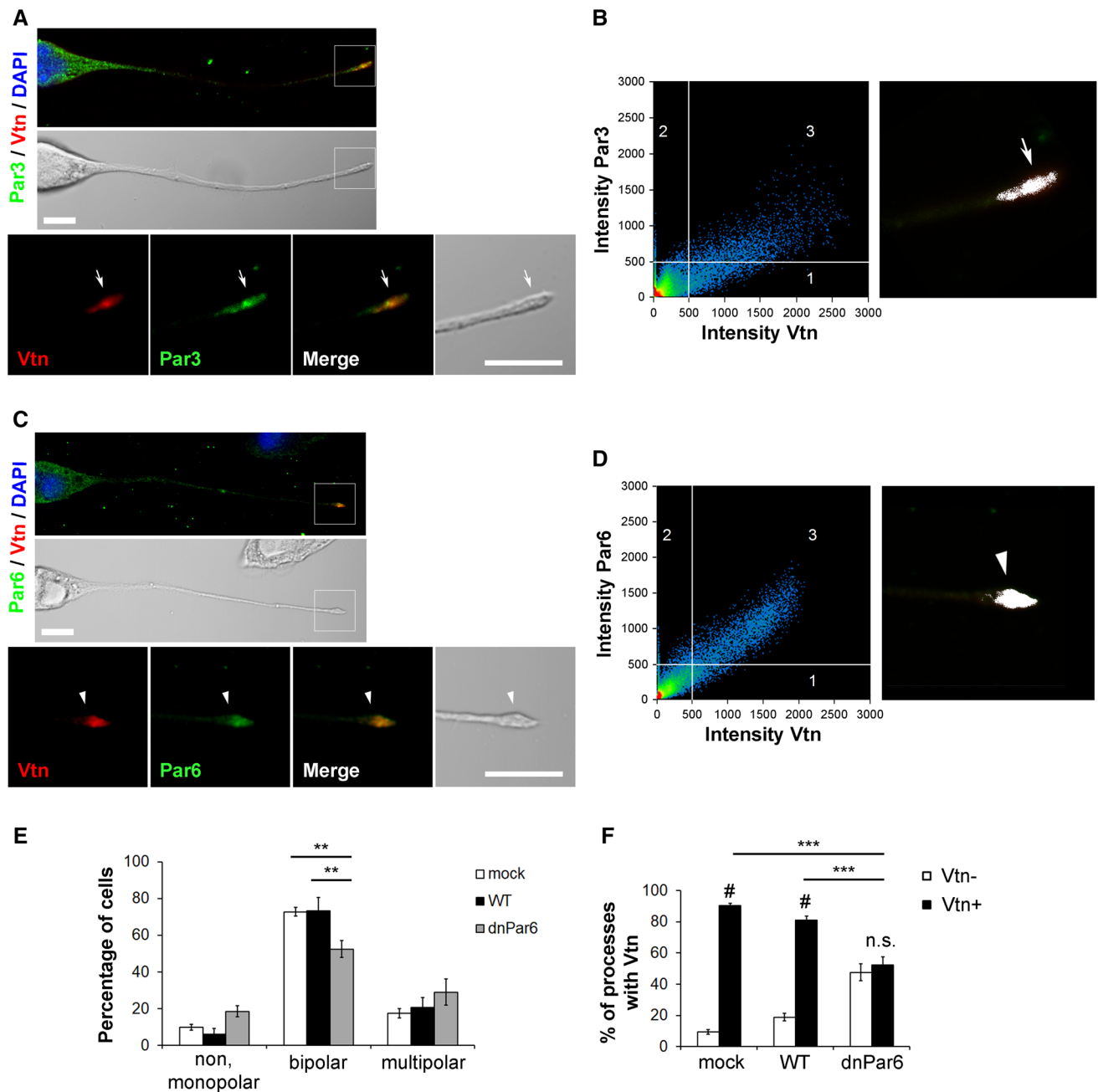
Fig. 4 Vtn interacts with the cell polarity regulator Par6 in RA-induced morphological transition of neurites. Cells (3.0×10^4 cells/well) were stimulated with 10 µM RA. Representative images of cells after immunofluorescence staining for Par3 (**a**) or Par6 (**c**). Par3 and Par6 are shown in green, Vtn in red and DAPI in blue. The lower panels are magnified images of neurite tips in the upper panels. Arrow in **a** and arrowhead in **c** indicates the location of Par3 and Par6 at the tip of neurite, respectively. Scale bar = 10 µm. Co-localization analysis of Vtn and Par3 (**b**) or Par6 (**d**). The Y-axis of the scattergram shows the fluorescence intensities of Par3 (**b**) or Par6 (**d**), and the X-axis shows that of Vtn. In the unlabeled quadrant in the lower left of the scattergram, the pixels are under the threshold values of both the fluorescence intensities of Vtn and Par3/Par6. In Quadrant 1, the pixels were beyond the threshold of the Vtn fluorescence intensities and under the threshold of Par3/Par6 fluorescence intensities. In Quadrant 2, the pixels were beyond the threshold of Par3/Par6 intensities and under the threshold of Vtn intensity. In Quadrant 3, the pixels were beyond the threshold of both Vtn and Par3/Par6 intensities, but were considered to be the regions of co-localization with Vtn and Par3/Par6. The right panel shows the pixels in Quadrant 3 displayed in fluorescence images in white to visualize the co-localization of Vtn and Par3/Par6. Effects of mutations in Par6 on neurite morphology (**e**) and localization of Vtn (**f**). Neuro2a cells were transfected with dominant negative Par6 (dnPar6), wild-type Par6 (WT), or empty vector plasmid (mock). The cells were stained with anti-flag and anti-Vtn antibodies. The neurites expressing Vtn at the tip were grouped into Vtn-positive (Vtn+) and Vtn-negative (Vtn−). Significance was calculated with ANOVA; **$p < 0.01$, ***$p < 0.001$. #significance between Vtn− and Vtn+. Data are mean ± SEM of three independent experiments (Color figure online)
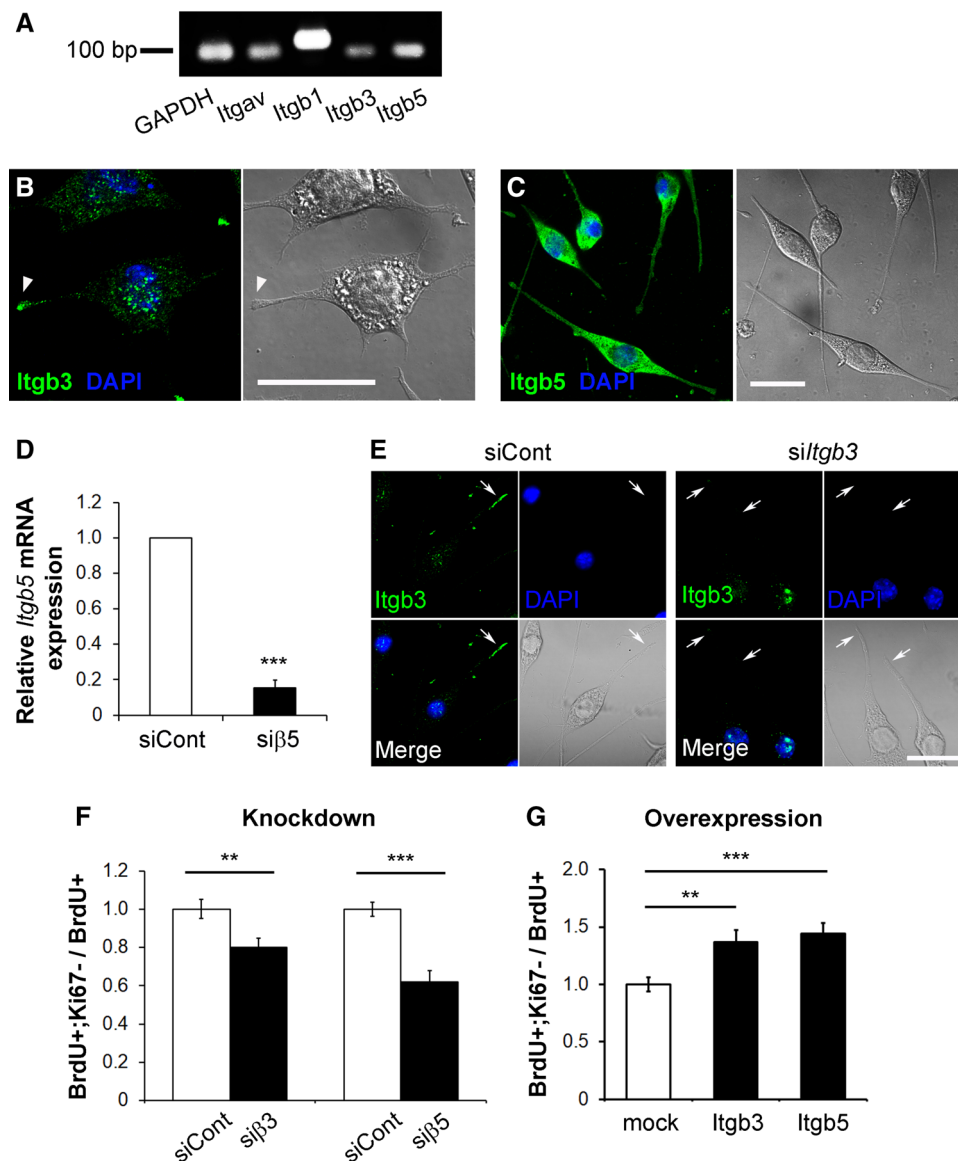
Fig. 5 Cell cycle exit is promoted by αvβ3 and αvβ5 integrins in Neuro2a cells. **a** RT-PCR of Vtn receptor candidates. Total RNA from Neuro2a cells after stimulation with 10 μM RA for 48 h was subjected to agarose gel electrophoresis. Representative images of cells after immunofluorescence staining for Itgb3 (green) (**b**) or Itgb5 (green) (**c**) and DAPI (blue). The arrowhead in **b** indicates the localization of Itgb3 at the tips of neurites. **d** Effect of knockdown on expression levels of *Itgb5* mRNA. cDNA was reverse-transcribed from mRNA isolated from Neuro2a cells stimulated with 10 μM RA for 48 h. Each mRNA level was quantified by real-time RT-PCR. Data were normalized to negative control siRNA (siCont)-transfected cells. Significance was calculated with unpaired t test. **e** Decrease in the expression levels of β3 integrin proteins by β3 integrin knockdown. Neuro2a cells were transfected with siRNA for *β3 integrin* (si*Itgb3*) or siCont and cultured with 10 μM RA for 48 h. Cells were stained with anti-Itgb3 antibody (green) and DAPI (blue). Arrows indicate the neurite tips where β3 integrin was localized. **f** The effect of integrin knockdown on cell cycle exit. Cells were transfected with the siRNA for β3 integrin (siβ3), β5 integrin (siβ5) or a negative-control siRNA (siCont), and stimulated with 10 μM RA for 48 h. **g** The effect of integrin overexpression on cell cycle exit. Cells were transfected with pCMV6-XL-β3 integrin (Itgb3), pCMV6-XL-β5 integrin (Itgb5), or pCMV6-XL expression vector plasmid (mock) and stimulated with 15 μM RA for 48 h. The efficiency of cell cycle exit is calculated as the percentage of cells that exited the cell cycle (BrdU+; Ki67−) divided by total BrdU-positive cells (BrdU+). The cells were labeled with BrdU for 24 h. Data were normalized to siCont or mock transfected cells. Significance was calculated with ANOVA; **$p < 0.01$, ***$p < 0.001$. Data are mean ± SEM of three independent experiments. Scale bar = 30 μm (Color figure online)

at neurite tips, while β5 integrin was detected ubiquitously in the cell.

Next, we performed knockdown experiments of β3 and β5 integrins. Transfection of *Itgb5* siRNA (β5 KD) significantly reduced the expression level of *Itgb5* mRNA to 15.4% of that in cells transfected with a negative-control siRNA (siCont) (Fig. 5d). Knockdown of β3 integrin (β3 KD) dissipated the localization of β3 integrin in the neurite tips (Fig. 5e). β3 KD and β5 KD significantly reduced the efficiency of the cell cycle exit by 20% and 38% of the siCont, respectively (Fig. 5f). In contrast, the overexpression of β3 and β5 integrins significantly increased the efficiency of the cell cycle exit to 130% and 140% of the siCont, respectively (Fig. 5g).

These results indicate that β3 and β5 integrins mediate the promotion of the cell cycle exit in the RA-stimulated Neuro2a cells.

Furthermore, we examined the effect of β3 KD and β5 KD on the morphological transition of neurites in Neuro2a cells (Fig. 6a). β3 KD suppressed the neurite elongation but did not affect the neurite morphology of RA-stimulated Neuro2a cells (Fig. 6b). β5 KD significantly reduced the ratio of bipolar (siCont: 66.3%, siβ5: 40.4%), and increased the ratio of cells with nonpolar and monopolar morphology (siCont: 17.0%, siβ5: 54.8% of total cell number) (Fig. 6c). To examine why β5 KD increases the ratio of cells with nonpolar and monopolar morphologies, we performed time-lapse imaging

Fig. 6 β5 integrin is involved in RA-induced morphological transition of neurites in Neuro2a cells. Cells (3.0×10^4 cells/well) were transfected with the siRNA for β3 integrin (siβ3), β5 integrin (siβ5) or a negative-control siRNA (siCont) and stimulated with 10 μM RA for 48 h. **a** Representative phase-contrast images of siCont, siβ3 and siβ5 cells. The effects of β3 (**b**) and β5 (**c**) integrin knockdown on the neurite morphological transition. **d** Time-lapse images of siCont and siβ5 cells. Images were obtained at 15-min intervals from 0 to 48 h after RA treatment. **e** the effects of β5 integrin knockdown on the neurite morphological transition at each time. The upper panel shows siCont cells, and the lower panel shows siβ5 cells. **f** Phase-contrast and Hoechst 33342 stained fluorescence images in siCont and siβ5 cells. The cell viability was determined from the perspective of nuclear morphology. Non-chromatin aggregation in the nuclei shows non-apoptotic cells (arrowheads), and chromatin aggregation in a nucleus shows apoptotic cells with non-polar morphology (arrow). **g** The effect of the β5 integrin knockdown on the cell viability. Significance was calculated with ANOVA; $*p < 0.05$, $**p < 0.01$, $***p < 0.001$. Data are mean ± SEM of three independent experiments. Scale bar = 50 μm
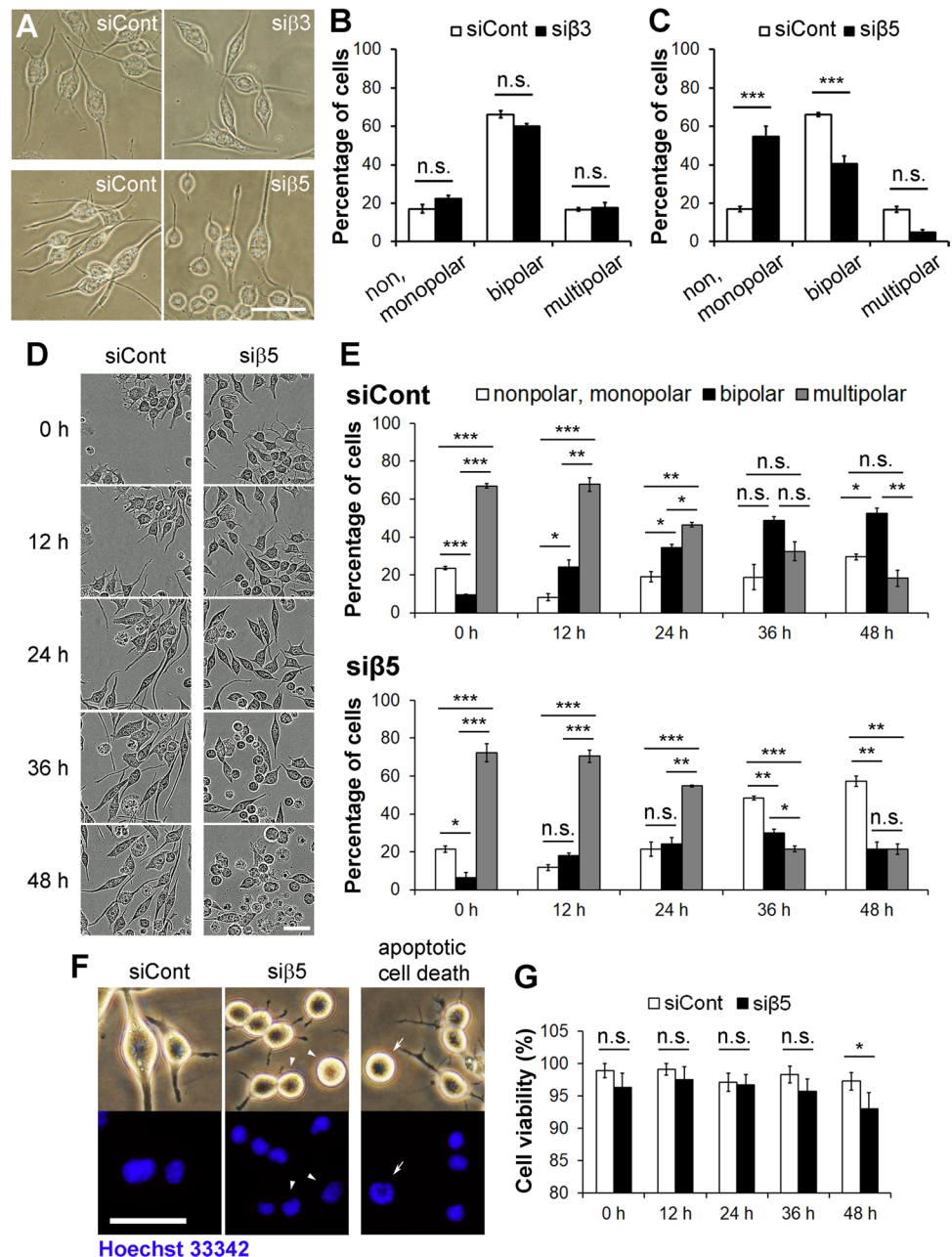
for 48 h after treatment with RA (Fig. 6d). In the control cells (siCont), the ratio of cells displaying multipolar morphology was decreased and that of cells displaying bipolar morphology was increased time-dependently (Fig. 6e). In contrast, in the β5 KD cells, the multipolar-to-bipolar transition was observed up to 24 h, similar to the control cells. However, after 36 h, β5 KD decreased the ratio of cells with multipolar morphology, and increased that of the cells with nonpolar/monopolar morphology (Fig. 6e). These data indicated that β5 KD induces a morphological transition from multipolar to nonpolar/monopolar after 36 h. To investigate whether cell death increased the ratio of nonpolar/monopolar morphology induced by β5 KD, cell viability was analyzed from the perspective of nuclear morphology using Hoechst staining. The results showed that the nuclei of most cells in β5 KD did not show chromatin aggregation, as seen in apoptotic cells (Fig. 6f). More than 95% of cells in β5 KD were alive, similar to control cells for up to 36 h, and viability was significantly decreased to approximately 90% at 48 h, compared with that of control cells (Fig. 6g).

αvβ5 Integrin Plays an Important Role as Vtn Receptor in Multipolar-to-Bipolar Transition of RA-Stimulated Neuro2a Cells

It is known that Vtn can bind to all αv integrins (e.g. αvβ1, αvβ3 and αvβ5 integrin) which have RGD recognition sites [26, 27]. Therefore, in order to examine whether αvβ3 and αvβ5 integrins serve as Vtn receptors, double knockdowns (KDs) of Vtn and β3 or β5 integrin were performed in RA-stimulated Neuro2a cells.

As a result, the double KDs of Vtn and β3 or β5 integrin remarkably suppressed the RA-induced cell cycle exit, but they could not be rescued by the addition of Vtn (Fig. 7a). The double KD of Vtn and β3 integrin reduced the ratio of cells with bipolar morphology (from 71.0 to 38.7% of the total cell number), and increased the ratio of cells with multipolar morphology (from 18.3 to 38.7% of the total cell number), compared with the siCont. Furthermore, the suppression of multipolar-to-bipolar transition by the double KD of Vtn and β3 integrin was rescued by Vtn addition (Fig. 7b). In contrast, the double KD of Vtn and β5 integrin remarkably reduced the ratio of cells with bipolar morphology (from 71.0 to 28.8% of total cell number) and increased the ratio of cells with nonpolar and monopolar morphology (from 10.8 to 51.6% of total cell number), compared with siCont. However, the perturbation of multipolar-to-bipolar transition could not be rescued with the addition of Vtn. These data indicate that β5 integrin contributes to the RA-induced multipolar-to-bipolar transition as a receptor for Vtn in Neuro2a cells.

Discussion

In this study, we aimed to identify the effect of Vtn and its integrin receptors on the multipolar-to-bipolar transition of neural progenitor cells. To address this research question, the mouse neuroblastoma cell line Neuro2a was used. RA treatment leads to cell cycle exit, polarization, and the morphological transition of neurites in Neuro2a cells. Our data revealed that Vtn regulates the RA-induced multipolar-to-bipolar transition through αvβ5 integrin, accompanying the
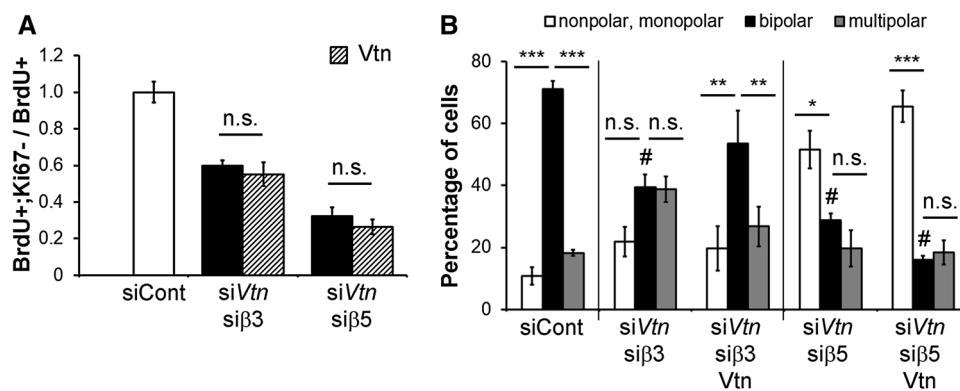

Fig. 7 αvβ3 and αvβ5 integrins serve as Vtn receptors. Cells (3.0×10⁴ cells/well) were transfected with the siRNA for Vtn (si*Vtn*) with β3 integrin (siβ3) or β5 integrin (siβ5) and stimulated by 10 µM RA for 48 h. To perform rescue experiments, Vtn protein (5 µg/ml) was added to the double knockdown cells (Vtn). **a** The effect of a double knockdown of Vtn and integrin on the cell cycle exit. The efficiency of the cell cycle exit is calculated as the percentage of cells that exited the cell cycle (BrdU+; Ki67−) divided by total

BrdU-positive cells (BrdU+). The cells were labeled with BrdU for 24 h. Data were normalized to siCont cells. **b** The effect of a double knockdown of Vtn and integrin on the neurite morphological transition. Significance was calculated with ANOVA; *$p < 0.05$, **$p < 0.01$, ***$p < 0.001$, #Significance based on the fraction of bipolar morphology in siCont cells. Data are mean ± SEM of three independent experiments

cell cycle exit and polarization related to Par6 in Neuro2a cells.

Vtn has been reported to regulate the differentiation, cell cycle exit, polarization, and neurite formation of neural progenitor cells in the developing nervous system and plays an important role in the neurogenesis of neural progenitor cells. For example, Vtn regulates the neurite elongation of neural retina and dorsal root ganglia, and differentiation of motor neurons and CGCPs [11, 12, 28–31]. Vtn regulates the position of the centrosome in polarizing cerebellar granule cells and contributes to the polarization of CGCPs [14]. However, the mechanism of the Vtn regulation of polarization and morphological transition from neural progenitor cells to neurites is not fully understood. Our findings show that Vtn was localized at more than two neurite tips in the cells with multipolar morphology and in neurite tips of cells with bipolar morphology (Fig. 3). These results suggest that Vtn-negative neurites degenerate and Vtn-positive neurites elongate during the RA-induced transition from the multipolar to bipolar morphology. These localizations of Vtn in the tips of neurites were suppressed by dominant negative Par6 (Fig. 4). In addition, the inhibition of Vtn with the anti-Vtn antibody and the overexpression of dominant negative Par6 suppressed the multipolar-to-bipolar transition (Figs. 3, 4). These results suggest that the multipolar-to-bipolar transition is involved in the localization of Vtn at the tip of the neurites and polarization of RA-stimulated Neuro2a cells. Since the mechanism by which Vtn localizes at the tip of neurites is still unknown, further research is needed to reveal how Vtn regulates the multipolar-to-bipolar transition during RA-induced neurogenesis in Neuro2a cells.

Neuro2a cells are widely used as a model of neuron-like differentiation such as neurite elongation and share similar properties as neural progenitor cells. For instance, adiponectin and pannexin-2 regulate the proliferation of both Neuro2a cells and hippocampal neural progenitor cells [32, 33]. Additionally, the multipolar-to-bipolar transition of neurites, which was evaluated in this study, has been reported in RA-treated Neuro2a cells [18]. Neuro2a cells are useful models for investigating the role of Vtn in the multipolar-to-bipolar transition of neurites. Similar to observations in the developing cerebellum, retina, and neural tube [8, 10, 12], our previous study showed that RA treatment transiently up-regulates the expression level of Vtn protein in the conditioned medium of Neuro2a cells [19]. In this study, we also observed up-regulation of *Vtn* mRNA and Vtn protein in the cell lysate of Neuro2a cells (Fig. 1). These results support that Vtn in Neuro2a cells can be used to evaluate the development of neural progenitor cells such as cell cycle exit and neurite morphological transition. Western blotting analysis of Vtn protein levels showed a Vtn band in Neuro2a cells which was slightly larger in molecular weight than that in the mouse plasma (Fig. 1a). This may be because of the

remaining signal peptide for the Vtn protein in the cell lysate of Neuro2a cells.

Knockdown experiments of β3 and β5 integrins (Figs. 6, 7) indicated that αvβ5 integrin, but not αvβ3 integrin, contributes to the regulation of Vtn on the RA-induced neurite morphological transition. Recently, we reported that αvβ5 integrin mediates the effect of Vtn on the initial stage of differentiation in mouse CGCPs [15]. The initial differentiation stage of CGCPs localized in the inner external granule cell layer is progressed where the transition of neurites from multipolar to bipolar morphology [5]. These findings support the notion that αvβ5 integrin serves as a receptor for Vtn during the RA-induced morphological transition in Neuro2a cells. However, the β5 KD decreased the fraction of bipolar morphology and increased the ratio of nonpolar and monopolar morphology to total cells (Fig. 6c). On the other hand, the inhibition of Vtn decreased the fraction of bipolar morphology and increased the ratio of multipolar morphology to total cells (Fig. 3g). This result apparently contradicts the results of the β5 KD. In comparison with the Vtn inhibition experiments (Fig. 3f), the phase-contrast images of the β5 KD show a round shape of cell bodies and short, thin neurites (Fig. 6a). This discrepancy may be due to the β5 KD induced collapse of neurite formation. This hypothesis is supported by the time-lapse images showing that β5 KD collapsed the multipolar neurites, which were observed from 12 h until 48 h after RA treatment (Fig. 6e). The quantitative analyses of the time-lapse images indicated that β5 KD induced a multipolar to nonpolar/monopolar transition. In addition, the incidence of cell death induced by β5 KD was only 10% of the total cells, which suggested that the contribution of the cell death to the multipolar to nonpolar/monopolar transition is low. Therefore, it was suggested that the knockdown of β5 integrin causes a multipolar to nonpolar/monopolar transition, mainly due to neurite collapse. The neurites may not have been collapsed by Vtn inhibition as other ligands may bind to αvβ5 integrin, thereby leading to multipolar morphology. Osteopontin has been reported to be a ligand candidate for αvβ5 integrin produced in Neuro2a cells [34, 35].

Our results also indicate a relationship between cell cycle exit and the morphological transition of neurites. The mechanism of this relationship may involve cyclin-dependent kinase inhibitor 1B (p27^{Kip1}). This protein is not only a cyclin-dependent kinase inhibitor that regulates cell cycle exit but also a regulator of the Rho kinase that regulates actin organization and potentially also regulates neurite morphology [4, 36, 37]. Additionally, p27^{Kip1} has been reported to regulate the cell cycle exit of neuronal progenitor cells coordinately with Rp58, which regulates the multipolar-to-bipolar transition of neurites in the developing mouse cerebral cortex [38]. Other studies reported that p35/cyclin-dependent kinase 5 (Cdk5) regulates not only cell cycle exit

but also neuronal morphology in the developing cerebral cortex [39, 40]. They reported that p35/Cdk5 is localized to the growth cone and affect neuronal morphology by regulating the neuronal cytoskeleton such as actin and tubulin. Furthermore, RA-responsive gene neuron navigator 2 (Nav2) interacts with microtubules to induce neurite outgrowth [41]. These studies indicate that p27^{Kip1}, Cdk5, and RA are involved in cell cycle exit and the morphological transition of neurites. Additionally, the results of knockdown experiments of β3 and β5 integrin showed that both integrins are involved in cell cycle exit, and only β5 integrin is involved in the morphological transition of neurites. These data support that the morphological transition of neurites is linked to cell cycle exit in the RA-stimulated Neuro2a cells.

In this study, our results demonstrate that αvβ3 and αvβ5 integrins have different roles in promoting Vtn-induced cell cycle exit and the morphological transition of neurites in Neuro2a cells. We recently reported that Vtn promotes the initial stage of differentiation in CGCPs via αvβ5 integrin [15, 16], whereas αvβ3 integrin has been reported to mediate the suppression of proliferation [42]. Although it has been reported that several integrins are involved in various stages of neuronal differentiation, the mechanism by which integrins exhibit different functions remains unclear. There are two possible hypotheses: first, the timing of the expression of each integrin is different; second, the localization of each integrin is different. Similarly, in oligodendrocyte precursor cells, four integrins are involved in different stages of differentiation, the time-dependent expression of each integrin is tightly controlled to ensure their functions [43, 44]. The different localization of β3 and β5 integrins (Fig. 5) may be due to their different functions in Neuro2a cells.

Our results show that the relationship between Vtn and Par6 (a cell polarity regulator) is involved in the RA-induced morphological transition of neurites in Neuro2a cells. It has been reported that polarity kinase 1 (Par1) is associated with the multipolar-to-bipolar transition of neuronal progenitor cells in the developing cerebral cortex [45]. This study shows that dnPar6 perturbed the multipolar-to-bipolar transition and Vtn localization at the tips of neurites (Fig. 4), suggesting that Par6 is related to the effect of Vtn on the RA-induced morphological transition of neurites. The localization of the Par complex at the neurite tips has been reported to control the dynamics of actin filaments with Cdc42 and Rac [46–49]. Neuro2a cells form neurites with F-actin-enriched protrusions when stimulated by RA [50]. These reports support that the Par complex is related to the RA-induced morphological transition in Neuro2a cells. In addition, it has been reported that Vtn is involved in polarization by regulating the centrosome configuration in cerebellar granule cells; a signaling pathway involving Par has been proposed as well [14]. Although the multipolar-to-bipolar transition

is an important event during the initial differentiation of the cerebrum and cerebellum, an extracellular factor which contributes to this event has not been identified yet. This study suggests that Vtn may be a potential candidate factor. Further investigations are expected to clarify the mechanism of Vtn involved in the morphological transition of neurites in neural progenitor cells.

In summary, this study indicates that Vtn contributes to RA-induced multipolar-to-bipolar transition, accompanied with cell cycle exit, through αvβ5 integrin in the mouse neuroblastoma cell line, Neuro2a. In addition, it was found that the multipolar-to-bipolar transition is regulated by the cell polarity regulator Par6 in Neuro2a cells.

Compliance with Ethical Standards

Conflict of interest The authors declare no conflict of interest.

Ethical Approval This article does not contain any studies with human participants or animals performed by any of the authors.

References

1. Miyata T, Ono Y, Okamoto M, Masaoka M, Sakakibara A, Kawaguchi A, Hashimoto M, Ogawa M (2010) Migration, early axonogenesis, and Reelin-dependent layer-forming behavior of early/posterior-born Purkinje cells in the developing mouse lateral cerebellum. Neural Dev 5:23
2. Lui JH, Hansen DV, Kriegstein AR (2011) Development and evolution of the human neocortex. Cell 146:18–36
3. Tabata H, Nakajima K (2003) Multipolar migration: the third mode of radial neuronal migration in the developing cerebral cortex. J Neurosci 23:9996–10001
4. Kawauchi T, Chihama K, Nabeshima Y, Hoshino M (2006) Cdk5 phosphorylates and stabilizes p27kip1 contributing to actin organization and cortical neuronal migration. Nat Cell Biol 8:17–26
5. Nakashima K, Umeshima H, Kengaku M (2015) Cerebellar granule cells are predominantly generated by terminal symmetric divisions of granule cell precursors. Dev Dyn 244:748–758
6. Seiffert D, Iruela-Arispe ML, Sage EH, Loskutoff DJ (1995) Distribution of vitronectin mRNA during murine development. Dev Dyn 203:71–79
7. Hayman EG, Pierschbacher MD, Ohgren Y, Ruoslahti E (1983) Serum spreading factor (vitronectin) is present at the cell surface and in tissues. Proc Natl Acad Sci USA 80:4003–4007
8. Martinez-Morales JR, Barbas JA, Marti E, Bovolenta P, Edgar D, Rodriguez-Tebar A (1997) Vitronectin is expressed in the ventral region of the neural tube and promotes the differentiation of motor neurons. Development 124:5139–5147

9. Pons S, Marti E (2000) Sonic hedgehog synergizes with the extracellular matrix protein vitronectin to induce spinal motor neuron differentiation. Development 127:333–342

10. Martinez-Morales JR, Marti E, Frade JM, Rodriguez-Tebar A (1995) Developmentally regulated vitronectin influences cell differentiation, neuron survival and process outgrowth in the developing chicken retina. Neuroscience 68:245–253

11. Grabham PW, Gallimore PH, Grand RJ (1992) Vitronectin is the major serum protein essential for NGF-mediated neurite outgrowth from PC12 cells. Exp Cell Res 202:337–344

12. Pons S, Trejo JL, Martinez-Morales JR, Marti E (2001) Vitronectin regulates Sonic hedgehog activity during cerebellum development through CREB phosphorylation. Development 128:1481–1492

13. Murase S, Hayashi Y (1998) Concomitant expression of genes encoding integrin alpha v beta 5 heterodimer and vitronectin in growing parallel fibers of postnatal rat cerebellum: a possible role as mediators of parallel fiber elongation. J Comp Neurol 397:199–212

14. Gupta SK, Meiri KF, Mahfooz K, Bharti U, Mani S (2010) Coordination between extrinsic extracellular matrix cues and intrinsic responses to orient the centrosome in polarizing cerebellar granule neurons. J Neurosci 30:2755–2766

15. Abe A, Hashimoto K, Akiyama A, Iida M, Ikeda N, Hamano A, Watanabe R, Hayashi Y, Miyamoto Y (2018) alphavbeta5 integrin mediates the effect of vitronectin on the initial stage of differentiation in mouse cerebellar granule cell precursors. Brain Res 1691:94–104

16. Hashimoto K, Sakane F, Ikeda N, Akiyama A, Sugahara M, Miyamoto Y (2016) Vitronectin promotes the progress of the initial differentiation stage in cerebellar granule cells. Mol Cell Neurosci 70:76–85

17. Marzinke MA, Clagett-Dame M (2012) The all-trans retinoic acid (atRA)-regulated gene Calmin (Clmn) regulates cell cycle exit and neurite outgrowth in murine neuroblastoma (Neuro2a) cells. Exp Cell Res 318:85–93

18. Mori Y, Matsui T, Omote D, Fukuda M (2013) Small GTPase Rab39A interacts with UACA and regulates the retinoic acid-induced neurite morphology of Neuro2A cells. Biochem Biophys Res Commun 435:113–119

19. Shimizu S, Kondo M, Miyamoto Y, Hayashi M (2002) Foxa (HNF3) up-regulates vitronectin expression during retinoic acid-induced differentiation in mouse neuroblastoma Neuro2a cells. Cell Struct Funct 27:181–188

20. Lee JY, Tsuchiya R, Miyamoto Y, Hayashi M (1998) A protein reacted with anti-vitronectin antibody accumulates in tumors derived from B16F10 melanoma cells. Cell Struct Funct 23:193–199

21. Boitard M, Bocchi R, Egervari K, Petrenko V, Viale B, Gremaud S, Zgraggen E, Salmon P, Kiss JZ (2015) Wnt signaling regulates multipolar-to-bipolar transition of migrating neurons in the cerebral cortex. Cell Rep 10:1349–1361

22. Shah B, Lutter D, Bochenek ML, Kato K, Tsytsyura Y, Glyvuk N, Sakakibara A, Klingauf J, Adams RH, Puschel AW (2016) C3G/Rapgef1 is required in multipolar neurons for the transition to a bipolar morphology during cortical development. PLoS ONE 11:e0154174

23. Barnat M, Le Friec J, Benstaali C, Humbert S (2017) Huntingtin-mediated multipolar-bipolar transition of newborn cortical neurons is critical for their postnatal neuronal morphology. Neuron 93:99–114

24. Etienne-Manneville S, Hall A (2003) Cell polarity: Par6, aPKC and cytoskeletal crosstalk. Curr Opin Cell Biol 15:67–72

25. Betschinger J, Knoblich JA (2004) Dare to be different: asymmetric cell division in Drosophila, C. elegans and vertebrates. Curr Biol 14:R674–685

26. DeSimone DW, Stepp MA, Patel RS, Hynes RO (1987) The integrin family of cell surface receptors. Biochem Soc Trans 15:789–791

27. Felding-Habermann B, Cheresh DA (1993) Vitronectin and its receptors. Curr Opin Cell Biol 5:864–868

28. Neugebauer KM, Emmett CJ, Venstrom KA, Reichardt LF (1991) Vitronectin and thrombospondin promote retinal neurite outgrowth: developmental regulation and role of integrins. Neuron 6:345–358

29. Isahara K, Yamamoto M (1995) The interaction of vascular endothelial cells and dorsal root ganglion neurites is mediated by vitronectin and heparan sulfate proteoglycans. Brain Res Dev Brain Res 84:164–178

30. Wang AG, Yen MY, Hsu WM, Fann MJ (2006) Induction of vitronectin and integrin alphav in the retina after optic nerve injury. Mol Vis 12:76–84

31. Katic J, Loers G, Kleene R, Karl N, Schmidt C, Buck F, Zmijewski JW, Jakovcevski I, Preissner KT, Schachner M (2014) Interaction of the cell adhesion molecule CHL1 with vitronectin, integrins, and the plasminogen activator inhibitor-2 promotes CHL1-induced neurite outgrowth and neuronal migration. J Neurosci 34:14606–14623

32. Yau SY, Li A, Hoo RL, Ching YP, Christie BR, Lee TM, Xu A, So KF (2014) Physical exercise-induced hippocampal neurogenesis and antidepressant effects are mediated by the adipocyte hormone adiponectin. Proc Natl Acad Sci USA 111:15810–15815

33. Swayne LA, Sorbara CD, Bennett SA (2010) Pannexin 2 is expressed by postnatal hippocampal neural progenitors and modulates neuronal commitment. J Biol Chem 285:24977–24986

34. Yokosaki Y, Tanaka K, Higashikawa F, Yamashita K, Eboshida A (2005) Distinct structural requirements for binding of the integrins alphavbeta6, alphavbeta3, alphavbeta5, alpha5beta1 and alpha-9beta1 to osteopontin. Matrix Biol 24:418–427

35. Morisaki Y, Niikura M, Watanabe M, Onishi K, Tanabe S, Moriwaki Y, Okuda T, Ohara S, Murayama S, Takao M, Uchida S, Yamanaka K, Misawa H (2016) Selective expression of osteopontin in ALS-resistant motor neurons is a critical determinant of late phase neurodegeneration mediated by matrix metalloproteinase-9. Sci Rep 6:27354

36. Godin JD, Thomas N, Laguesse S, Malinouskaya L, Close P, Malaise O, Purnelle A, Raineteau O, Campbell K, Fero M, Moonen G, Malgrange B, Chariot A, Metin C, Besson A, Nguyen L (2012) p27(Kip1) is a microtubule-associated protein that promotes microtubule polymerization during neuron migration. Dev Cell 23:729–744

37. Hnit SS, Xie C, Yao M, Holst J, Bensoussan A, De Souza P, Li Z, Dong Q (2015) p27(Kip1) signaling: transcriptional and post-translational regulation. Int J Biochem Cell Biol 68:9–14

38. Clement O, Hemming IA, Gladwyn-Ng IE, Qu Z, Li SS, Piper M, Heng JI (2017) Rp58 and p27(kip1) coordinate cell cycle exit and neuronal migration within the embryonic mouse cerebral cortex. Neural Dev 12:8

39. Rashid T, Banerjee M, Nikolic M (2001) Phosphorylation of Pak1 by the p35/Cdk5 kinase affects neuronal morphology. J Biol Chem 276:49043–49052

40. Cicero S, Herrup K (2005) Cyclin-dependent kinase 5 is essential for neuronal cell cycle arrest and differentiation. J Neurosci 25:9658–9668

41. Muley PD, McNeill EM, Marzinke MA, Knobel KM, Barr MM, Clagett-Dame M (2008) The atRA-responsive gene neuron navigator 2 functions in neurite outgrowth and axonal elongation. Dev Neurobiol 68:1441–1453

42. Le Dreau G, Nicot A, Benard M, Thibout H, Vaudry D, Martinerie C, Laurent M (2010) NOV/CCN3 promotes maturation of cerebellar granule neuron precursors. Mol Cell Neurosci 43:60–71

43. Milner R, Frost E, Nishimura S, Delcommenne M, Streuli C, Pytela R, Ffrench-Constant C (1997) Expression of alpha vbeta3 and alpha vbeta8 integrins during oligodendrocyte precursor differentiation in the presence and absence of axons. Glia 21:350–360

44. Blaschuk KL, Frost EE, ffrench-Constant C (2000) The regulation of proliferation and differentiation in oligodendrocyte progenitor cells by alphaV integrins. Development 127:1961–1969

45. Sapir T, Sapoznik S, Levy T, Finkelshtein D, Shmueli A, Timm T, Mandelkow EM, Reiner O (2008) Accurate balance of the polarity kinase MARK2/Par-1 is required for proper cortical neuronal migration. J Neurosci 28:5710–5720

46. Lin D, Edwards AS, Fawcett JP, Mbamalu G, Scott JD, Pawson T (2000) A mammalian PAR-3-PAR-6 complex implicated in Cdc42/Rac1 and aPKC signalling and cell polarity. Nat Cell Biol 2:540–547

47. Ohno S (2001) Intercellular junctions and cellular polarity: the PAR-aPKC complex, a conserved core cassette playing fundamental roles in cell polarity. Curr Opin Cell Biol 13:641–648

48. Etienne-Manneville S, Hall A (2002) Rho GTPases in cell biology. Nature 420:629–635

49. Goldstein B, Macara IG (2007) The PAR proteins: fundamental players in animal cell polarization. Dev Cell 13:609–622

50. Xiao Y, Peng Y, Wan J, Tang G, Chen Y, Tang J, Ye WC, Ip NY, Shi L (2013) The atypical guanine nucleotide exchange factor Dock4 regulates neurite differentiation through modulation of Rac1 GTPase and actin dynamics. J Biol Chem 288:20034–20045